1282 *Inorg. Chem.* **1999,** *38,* 1282−1287

New SO_2 Iron-Containing Cluster Compounds $[PPN]_2[Fe_3(CO)_9(\mu_3,\eta^2\text{-}SO_2)]$, $[PPN]_2[Fe_3(CO)_8(\mu\text{-}SO_2)\mu_3\text{-}S]$, $[PPN]_2[Fe_3(CO)_8(\mu\text{-}SO_2)(\mu_3\text{-}CCO)]$, and $[PPN]_2[Fe_2(CO)_6(\mu\text{-}SO_2)_2]$ from Heterometal Precursors

R. W. Eveland, C. C. Raymond, T. E. Albrecht-Schmitt, and D. F. Shriver*

Northwestern University, Department of Chemistry, Evanston, Illinois 60208

Received July 2, 1998

Sulfur dioxide reacts with $[PPN]_2[MFe_3(CO)_{14}]$ (M = Cr, Mo, W) (PPN = bistriphenylphosphonium iminium) to produce $[PPN]_2[Fe_3(CO)_9(\mu_3,\eta^2\text{-}SO_2)]$ (**I**) and $[PPN]_2[Fe_3(CO)_8(\mu\text{-}SO_2)\mu_3\text{-}S]$ (**II**), which were characterized by infrared spectroscopy, ^{13}C NMR, and X-ray crystallography. Further reaction of **I** with sulfur dioxide results in the formation of **II** in 48% yield. Reaction of SO_2 with $[PPN]_2[Fe_4(CO)_{13}]$ yields $[PPN]_2[Fe_2(CO)_6(\mu\text{-}SO_2)_2]$ (**III**) which was characterized by infrared spectroscopy, ^{13}C NMR, mass spectrometry, and X-ray crystallography. One equivalent of sulfur dioxide with $[PPN]_2[MFe_3(CO)_{14}C]$ (M = Cr, W) produces $[PPN]_2[Fe_3(CO)_8(\mu\text{-}SO_2)(\mu_3\text{-}CCO)]$ (**IV**), which on further reaction with SO_2 gives the known cluster $[PPN]_2[Fe_3(CO)_7(\mu\text{-}SO_2)_2(\mu_3\text{-}CCO)]$ (**V**). An excess of sulfur dioxide with $[MFe_3(CO)_nC]^{x-}$ (M = Cr, W: $n = 13$, $x = 2$; M = Rh: $n = 12$, $x = 1$; M = Mn: $n = 13$, $x = 1$) produced **V** as the only identified product. Crystallographic data for $\mathbf{I}\cdot 0.5CH_2Cl_2$: monoclinic, *Cc* (no. 9), $a = 29.7648(3)$ Å, $b = 14.6496(1)$ Å, $c = 21.7620(3)$ Å, $\beta = 123.397(1)°$, $V = 7922.3$ Å^3; $Z = 4$. Crystallographic data for $\mathbf{III}\cdot NCCH_3$: monoclinic $P2_1$ (no. 4), $a = 10.0295(5)$ Å, $b = 26.356(1)$ Å, $c = 14.1032(7)$ Å, $\beta = 94.691°$, $V = 3715.6(3)$ Å^3; $Z = 4$.

Introduction

Sulfur dioxide is a π-acid ligand that reacts with many metal carbonyl compounds to give sulfur dioxide complexes.[1−3] An interesting feature of this chemistry is the variety and number of bonding modes which SO_2 can adopt, including η^1-pyramidal, $[IrCl(CO)(PPh_3)_2(SO_2)]$,[4,5] η^1 planar $[OsHCl(CO)(PCy_3)_2(SO_2)]$, and η^2 in $[Rh(NO)(SO_2)(PPh_3)_2]$.[6] When two or more metals are present, SO_2 can bridge a metal−metal bond or form a bridge between metal centers that are not supported by a metal−metal bond. Sulfur dioxide may bridge metal atoms through both sulfur and oxygen as with $[Mo(CO)_2(PPh_3)(py)(\mu\text{-}SO_2)]_2$.[7] A few heterometallic SO_2-containing clusters are known, such as the late d-block clusters $[Os_3Pt(\mu\text{-}H)_2(\mu\text{-}SO_2)(CO)_{10}(PCy_3)]$[8] and $[Pt_3Au_2Cl(SO_2)_2(PCy_3)_3(P\{p\text{-}C_6H_4F\}_3)]$.[9]

The goals of the present research were to explore the synthesis and structures of new metal cluster compounds formed by the interaction of sulfur dioxide with metal carbonyl clusters, and the reactions of sulfur dioxide ligands in these clusters. The reactivity of the SO_2 ligand has been reviewed,[10] with emphasis on the reduction of coordinated SO_2 to other sulfur oxides or elemental sulfur.[11−15] Recent results in this laboratory show that the acylation of an S−O bond in $[HFe_3(CO)_9(\mu_3,\eta^2\text{-}SO_2)]^{1-}$ followed by reduction with $NaPh_2CO$ causes cleavage of an S−O bond and produces SO and S containing clusters (eq 1).[16]

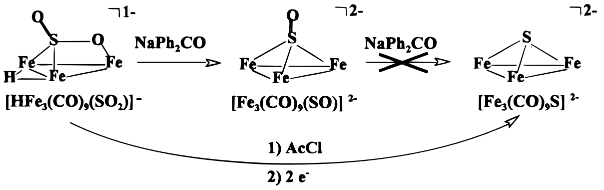

(1)

In the present research we explored the reaction of SO_2 with heterometallic carbonyl clusters, $[MFe_3(CO)_{14}]^{2-}$ (M = Cr, Mo, W), and heterometallic carbide clusters $[MFe_3(CO)_nC]^{x-}$ (M = Mn, Cr, W, Rh) with the thought that new types of metal reactivity might result.

Experimental Section

General Procedures and Materials. All manipulations were carried out with standard Schlenk techniques under a prepurified N_2 atmosphere or on a high vacuum line. Solids were handled in the oxygen-free N_2 atmosphere of a drybox. Solvents were distilled from appropriate drying agents before use. Solutions of the starting metal complex were freeze−pump−thaw degassed three times before SO_2 was introduced on a high vacuum line; the sulfur dioxide was used as received from Matheson. Infrared spectra were recorded on a Bomem MB-Series FTIR spectrometer at 2 cm^{-1} resolution. Solution spectra were obtained in matched

---

(1) Schenk, W. A. *Angew. Chem., Int Ed. Engl.* **1987**, *26*, 98−109.
(2) Mingos, D. M. P. *Trans. Met. Chem. (London)* **1978**, *3*, 1−15.
(3) Ryan, R. R.; Kubas, G. J. *Struct. Bonding Berlin* **1981**, *46*, 47.
(4) Vaska, L. *Acc. Chem. Res.* **1968**, *1*, 335.
(5) La Placa, S. J.; Ibers, J. A. *Inorg. Chem.* **1966**, *5*, 405.
(6) Moody, D. C.; Ryan, R. R. *Inorg. Chem.* **1977**, *16*, 2473.
(7) Jarvinen, G. D.; Kubas, G. J.; Ryan, R. R. *J. Chem. Soc., Chem. Com.* **1981**, *7*, 305−6.
(8) Ewing, P.; Farrugia, L. J. *Organometallics* **1989**, *8*, 1665−73.
(9) Mingos, D. M. P.; Oster, P.; Sherman, D. J. *J. Organomet. Chem.* **1987**, *320*, 257−66.
(10) Kubas, G. J. *Acc. Chem. Res.* **1994**, *27*, 183−90.
(11) Lang, R. F.; Ju, T. D.; Hoff, C. D.; Bryan, J. C.; Kubas, G. J. *J. Am. Chem. Soc.* **1994**, *116*, 9747−8.
(12) Kubas, G. J.; Ryan, R. R. *Inorg. Chem.* **1984**, *23*, 3181−3.
(13) Kubas, G. J.; Ryan, R. R. *J. Am. Chem. Soc.* **1985**, *107*, 6138−40.
(14) Karet, G. B.; Stern, C. L.; Cody, J. A.; Lange, S. J.; Pell, M. A.; Slebodnick, C.; Shriver, D. F. *J. Organomet. Chem.* **1995**, *495*, 33−39.
(15) Bogdan, P. L.; Sabat, M.; Sunshine, S. A.; Woodcock, C.; Shriver, D. F. *Inorg. Chem.* **1988**, *27*, 1904−10.
(16) Karet, G. B.; Stern, C. L.; Norton, D. M.; Shriver, D. F. *J. Am. Chem. Soc.* **1993**, *115*, 5, 9979−85.

10.1021/ic980762j CCC: \$18.00

air-free cells with CaF_2 windows; solid samples were prepared as Nujol mulls between KBr plates. Gaseous products were analyzed by infrared spectroscopy in a 10 cm gas cell with KBr windows. Raman spectra were recorded with a Bio-Rad FT Raman Spectrometer operating at 1064 nm excitation. The ^1H and ^{13}C NMR spectra were acquired on a Varian Unity 400+ spectrometer operating at 400 MHz for ^1H and 100 MHz for ^{13}C. CD_2Cl_2 was dried over P_2O_5 and was used as an internal standard. Mass spectra were determined at Washington University Mass Spectrometry Resource (St. Louis MO) or by Northwestern University Analytical Services Laboratory. Elemental analyses were performed by Elbach Analytical Laboratories, Engelskirchen, Germany.

The clusters $[PPN]_2[MFe_3(CO)_{14}]$ (M = Cr, Mo, W), $[PPN]_2[WFe_3(CO)_{13}C]$, $[PPN]_2[CrFe_3(CO)_{13}C]$, $[PPN][MnFe_3(CO)_{13}C]$, $[PPN][RhFe_3(CO)_{12}C]$, $[PPN]_2[Fe_4(CO)_{13}]$, $[PPN]_2[Fe_3(CO)_7(SO_2)_2(CCO)]$, $[PPN]_2[Fe_5(CO)_{13}(SO_2)]$, $[PPN]_2[Fe_6(CO)_{15}C(SO_2)]$, $[PPN][HFe_3(CO)_9(SO_2)]$, $[PPN]_2[Fe_3(CO)_9(SO)]$, $[PPN]_2[Ru_3(CO)_9(SO_2)]$, and $[PPN]_2[Ru_3(CO)_9(SO_2)_3]$ were prepared by published procedures.[14−16,18−20] ($[PPN]^+$ is bis(triphenylphosphine)iminium.) Trifluoromethanesulfonic acid (HSO_3CF_3, HOTf) was purchased from Aldrich and used without further purification.

Reaction of $[PPN]_2[MFe_3(CO)_{14}]$ (M = W, Cr, Mo) 1:1 with SO_2. Sulfur dioxide (2.53×10^{-4} mol) was condensed onto a frozen solution containing 0.399 g (2.19×10^{-4} mol) of $[PPN]_2[WFe_3(CO)_{14}]$ in 10 mL of CH_2Cl_2. The solution was warmed to room temperature and stirred for 3 h. Gaseous products were collected by low-temperature condensation and identified by infrared spectroscopy as CO_2 and CO. Solvent was removed under vacuum, and $W(CO)_6$ was removed by sublimation. The remaining products were separated from the reaction mixture by dissolution of the solids in 10 mL of THF followed by addition of 20 mL of Et_2O, which resulted in formation of red solids and a light red solution. The red solution was removed by filtration. This process was repeated three times. The solid product consisted primarily of $[PPN]_2[Fe_3(CO)_9(SO_2)]$ (**I**), which forms red, platelike crystals from 5:1 Et_2O/ CH_2Cl_2 (41% yield based on iron). Solvent was removed from the filtrate to produce a brown solid, which was dissolved in acetone. Subsequent slow diffusion of pentane into this solution yielded red-brown crystals of the new compound $[PPN]_2[Fe_3(CO)_8(SO_2)S]$ (**II**) (18% yield based on iron). Similar procedures were used for the reaction of SO_2 with $[PPN]_2[MoFe_3(CO)_{14}]$ and $[PPN]_2[CrFe_3(CO)_{14}]$, where **I** and **II** were the products.

Infrared spectra for $[PPN]_2[Fe_3(CO)_9(SO_2)]$ (**I**) reveal ν_{CO} (CH_2Cl_2) 2016(w), 1947(vs), 1920(m), 1782(w, br) cm^{-1}; ν_{CO} (THF) 2011(w), 1939(vs), 1916(m), 1785(w, br) cm^{-1}; ν_{CO} (Nujol) 2011(m), 1958(sh), 1938(vs), 1913(s), 1783(w, br) cm^{-1}, and ν_{SO} at 1162 and 902 cm^{-1}. An electrospray mass spectrum of **I** displayed a parent peak at 483 *m*/*z* and additional peaks corresponding to successive loss of four CO ligands. ^{13}C NMR spectra were collected from 20 to −80 °C in CD_2Cl_2, and the chemical shifts at 20 °C showed terminal carbonyls at 225.76 and 221.61 ppm. Elemental analysis of **I**: Calcd (Found) for $C_{81}H_{60}N_2Fe_3SO_{11}P_4$: C 62.3 (62.1), H 3.87 (3.71), N 1.79 (1.75).

The infrared spectra for CH_2Cl_2 solutions of $[PPN]_2[Fe_3(CO)_8(SO_2)S]$ (**II**) contain CO stretching bands at 2011(m), 1964(s), 1916(vs), 1842(m) cm^{-1}. In mulls the CO frequencies are 1996, 1961, 1908, 1841 cm^{-1}, and ν_{SO} at 1066 cm^{-1}. The electrospray mass spectrum of **II** contains a parent peak at 487 *m*/*z* and lower mass peaks corresponding to the successive loss of three CO ligands. The ^{13}C NMR spectra of **II** were collected from 20 to −60 °C in CD_2Cl_2. Chemical shifts at −60 °C were observed at 200.97, 198.65, 198.01, 197.38 (terminal CO), and 190.65 (μ-CO) ppm. Elemental analysis of **II**: Calcd (Found) for $C_{80}H_{60}N_2Fe_3P_4O_{10}S_2$: C 62.61 (62.01), H 3.86 (3.80), N 1.83 (1.80), S 4.18 (4.12).

Reaction of $[PPN]_2[MFe_3(CO)_{14}]$ (M = W, Cr, Mo) with Excess SO_2. Sulfur dioxide (5.80×10^{-4} mol) was condensed onto a frozen solution containing 0.252 g (1.38×10^{-4} mol) of $[PPN]_2[WFe_3(CO)_{14}]$ in 15 mL of CH_2Cl_2. The solution was warmed to room temperature and stirred overnight. Carbon dioxide was identified as a gaseous reaction product. The iron-containing products of this reaction, **I** and **II**, were separated and purified as described above. Similar procedures were used for the reaction of SO_2 with $[PPN]_2[MoFe_3(CO)_{14}]$ and $[PPN]_2[CrFe_3(CO)_{14}]$.

Reaction of $[PPN]_2[Fe_4(CO)_{13}]$ with SO_2. Sulfur dioxide (7.58×10^{-4} mol) was condensed onto a frozen solution containing 0.278 g (1.67×10^{-4} mol) of $[PPN]_2[Fe_4(CO)_{13}]$ in 15 mL of CH_2Cl_2. As the solution warmed to room temperature, the color changed from red to red-brown and gas was evolved. The solution was stirred overnight, and both carbon monoxide and carbon dioxide were identified as gaseous products by their IR spectra. Solvent was removed under vacuum, and the solids were redissolved in 10 mL of CH_3CN, and subsequent addition of 70 mL of Et_2O with vigorous stirring gave a red solid and a red-brown solution which were separated by filtration. The vacuum-dried red solid was redissolved in 7 mL of CH_3CN and layered with 50 mL of Et_2O. Ruby-red crystals of $[PPN]_2[Fe_2(CO)_6(SO_2)_2]$ (**III**) resulted (ca. 10% yield).

Infrared spectra for $[PPN]_2[Fe_2(CO)_6(SO_2)_2]$ (**III**) revealed ν_{CO} (CH_2Cl_2) 2021(s), 1993(vs), 1981(vs), 1953(vs) cm^{-1}, and ν_{SO} at 1018 cm^{-1}; ν_{CO} (Nujol) 1996, 1986, 1941 cm^{-1}, and ν_{SO} at 1017 cm^{-1}. The electrospray mass spectrum displays a parent peak at 408.7 *m*/*z* for **III** + H. Elemental analysis **III**: Calcd for $Fe_2S_2P_4N_2C_{78}O_{10}H_{60}$ (Found) C 63.09(62.83); H 4.07 (3.91); N 1.89 (2.04); S 4.32 (4.50). A ^{13}C NMR of an enriched sample of **III** shows a single peak at 155.5 ppm at 20 °C.

Reaction of $[PPN]_2[Fe_3(CO)_9(SO_2)]$ (I) with HSO_3CF_3. A 1.30 μL aliquot (1.47×10^{-5} mol) of HSO_3CF_3 was added to a solution of 23.0 mg (1.47×10^{-5} mol) $[PPN]_2[Fe_3(CO)_9(SO_2)]$ in 5 mL of CH_2Cl_2. The color of the solution immediately changed from ruby-red to brown, and infrared spectra indicated the formation of the known compound $[PPN][HFe_3(CO)_9(SO_2)]$ (**VI**)[16] in quantitative yield.

Reaction of $[PPN]_2[Fe_3(CO)_9(SO_2)]$ with 1 SO_2. Sulfur dioxide (8.04×10^{-5} mol) was condensed onto a frozen solution containing 0.116 mg (7.46×10^{-5} mol) of $[PPN]_2[Fe_3(CO)_9(SO_2)]$ in 10 mL of CH_2Cl_2. The solution was warmed to room temperature and stirred for 3 h, and CH_2Cl_2 was removed under vacuum. Carbon dioxide was identified as the gaseous reaction product by IR spectroscopy. $[PPN]_2[Fe_3(CO)_8(SO_2)S]$ (**II**) (0.0562 g, 48% yield based on iron) was separated from the remaining solids by repeated dissolution of the crude product in 5 mL portions of THF followed by addition of 10 mL of Et_2O to precipitate solids which were then removed by filtration. The solid was collected and dried under vacuum to give **II**.

Reaction of $[PPN]_2[WFe_3(CO)_{13}C]$ with 1 SO_2. Sulfur dioxide (1.61×10^{-4} mol) was condensed onto a frozen solution containing 0.260 g (1.46×10^{-4} mol) of $[PPN]_2[WFe_3(CO)_{13}C]$ in 20 mL of CH_2Cl_2. The mixture was warmed to room temperature, stirred for 2 h, reduced to 5 mL under vacuum, and crystallized by addition of 40 mL of Et_2O followed by vigorous shaking to give red-brown solids and a light red-brown solution. The solids were collected by filtration and redissolved in 10 mL of THF, and this solution was layered with 60 mL of Et_2O to give long, thin red plates of the new compound $[PPN]_2[Fe_3(CO)_8(SO_2)(CCO)]$ (**IV**). Tungsten hexacarbonyl was identified in the filtrate.

Infrared spectra for $[PPN]_2[Fe_3(CO)_8(SO_2)(CCO)]$ (**IV**) show ν_{CO} (CH_2Cl_2) 2036 (s), 1985 (vs), 1948 (vs), 1908 (s),1805 (w), 1774 (w) cm^{-1}, and ν_{SO} at 1020 cm^{-1}; ν_{CO} (Nujol) 2033, 1978, 1950, 1894, and 1760 cm^{-1}, and ν_{SO} at 1064 and 1025 cm^{-1}. The FAB mass spectrum displays a parent peak at 497 *m*/*z* and peaks for progressive loss of four CO ligands. The ^{13}C NMR spectra was obtained in $CD_2Cl_2/CFCl_3$ from 25 to −120 °C, and the chemical shifts at −40 °C were δ 272.5 (2) (m-CO); 216.4, 210.1, 215.6, 213.1 (1:1:2:2) (terminal COs); 165.6 (*C*CO); and 2.2 ppm (C*C*O). Elemental analysis calcd (found) for $C_{82}H_{60}N_2Fe_3SP_4O_{11}$: C, 62.62 (62.34); H, 3.84 (4.02); N, 1.78 (1.85); Fe, 10.65 (10.65); S, 2.04 (2.10).

Similar procedures were employed in the reaction of $[PPN]_2[CrFe_3(CO)_{13}C]$ with 1 equiv of SO_2 to produce $Cr(CO)_6$ and **IV**. $[PPN][RhFe_3$-

---

(17) Kubas, G. J.; Wasserman, H. J.; Ryan, R. R. *Organometallics* **1985**, *4*, 2012−21.

(18) Horwitz, C. P.; Holt, E. M.; Shriver, D. F. *Inorg. Chem.* **1983**, *23*, 2491−9.

(19) Hriljac, J. A.; Holt, E. M.; Shriver, D. F. *Inorg. Chem.* **1987**, *26*, 2943−9.

(20) Whitmire, K.; Ross, J.; Cooper, C. B. I.; Shriver, D. F. *Inorg. Synth.* **1982**, *21*, 66−9.

Table 1. Crystal Data for $[PPN]_2[Fe_3(CO)_9(SO_2)]\cdot 0.5CH_2Cl_2$ and $[PPN]_2[Fe_2(CO)_6(SO_2)_2]\cdot 1NCCH_3$ (**III**)[a]

formula	$C_{81}H_{61}N_2O_{11}P_4SClFe_3$	$C_{80}H_{63}N_3O_{10}P_4S_2Fe_2$
formula weight	1603.26	1526.0
a	29.7648(3)	10.0295(5)
b	14.6496(1)	26.356(1)
c	21.7620(3)	14.1032(7)
α	90	90
β	123.397(1)	94.691(1)
γ	90	90
V (Å^3)	7922.3(2)	3715.6(3)
space group, Z *Cc*	*Cc*, 4	$P2_1$, 4
T (°C)	25	−178
λ (Å)	0.71073	0.71073
ρ_{calcd} (g cm^{-3})	1.344	1.364
μ (mm^{-1})	0.742	0.594
R1	0.0505	0.0684
wR2	0.1180	0.1756

[a] $R1 = (\sum||F_o| - |F_c||)/\sum|F_o|$, $wR2 = [(\sum w(F_o2 - F_c2)^2)/\sum w(F_o2)^2]^{1/2}$, $w = 1/[\sigma^2(F_o2) + (z_1,P)^2 + z_2P]$ where $P = (F_o2 + 2F_c2)/3$, z_1, z_2 = weighting and extra extinction.

$(CO)_{12}C]$ and $[PPN][MnFe_3(CO)_{13}C]$ do not react with one equivalent of SO_2 after stirring for 2 days at room temperature.

Reaction of $[PPN]_2[WFe_3(CO)_{13}C]$ with Excess SO_2. Sulfur dioxide (4.14×10^{-4} mol) was condensed onto a frozen solution containing 0.136 g (7.54×10^{-5} mol) $[PPN]_2[WFe_3(CO)_{13}C]$ in 10 mL of CH_2Cl_2. The solution was warmed to room temperature and stirred for 2 h. An infrared spectrum taken at this time indicated the presence of the known compound $[PPN]_2[Fe_3(CO)_7(SO_2)_2(CCO)]$ (**V**) in apparently quantitative yield.

Reaction of $[PPN][RhFe_3(CO)_{12}C]$, $[PPN]_2[CrFe_3(CO)_{13}C]$, or $[PPN][MnFe_3(CO)_{13}C]$ with excess SO_2 gave **V** as the only identified iron-containing product. The reaction times used were 9, 18, and 48 h, respectively.

Reaction of $[PPN]_2[Fe_3(CO)_8(SO_2)(CCO)]$ (IV) with 1 SO_2. Sulfur dioxide (1.20×10^{-5} mol) was added to a frozen solution containing 0.0160 g (1.01×10^{-5} mol) of **IV** in 10 mL of CH_2Cl_2. The solution was warmed to room temperature and stirred for 2 h. Infrared spectra indicate that the reaction went cleanly and completely to the bis-SO_2 product **V**.

Reaction of $[PPN]_2[Fe_4(CO)_{13}C]$ with 1 SO_2. Sulfur dioxide (1.55×10^{-5} mol) was added to 0.0216 g (1.29×10^{-5} mol) of $[PPN]_2[Fe_4(CO)_{13}C]$ in 5 mL of CH_2Cl_2. The solution was warmed to room temperature and stirred for 2 h. An IR spectrum showed only starting material and bis-SO_2 product **V**, with no evidence for the presence of the mono-SO_2 species **IV**.

Structure Determination of $[PPN]_2[Fe_3(CO)_9(SO_2)]$ (I)$\cdot 0.5CH_2Cl_2$. A clear, dark red, pyramidal crystal was mounted on a glass fiber with epoxy resin, and data were collected at room temperature, because the crystals crack at low temperature. A complete hemisphere of data was collected on a Siemens SMART-CCD diffractometer. The intensity data was collected with 30 s frame times and interpreted with SAINT.[21] The initial unit cell parameters were determined from several frames of data, but were redetermined using all of the unique data, Table 1. The structure was solved and refined using SHELXTL, and an absorption correction was performed using SADABS.[22,23] Hydrogen atoms were placed in idealized positions and refined with a riding model. Because of the method used by SADABS, no transmission factors are reported for the corrected data. The systematic absences indicate a C-centered monoclinic cell, containing a c-glide. Initial structure refinements in *Cc*(no. 9) proceeded smoothly, but there were 16 systematic absence violations (all of which are weak reflections with large standard deviations). Because of these violations and the "perils of *Cc*"[24,25] a closer inspection of the data was made, which showed that the cell did not have higher symmetry. Also, the structure did not refine properly in *C*2/*c* (no. 15). A check of the Flack parameters indicated the correct absolute structure.[26]

Structure Determination for $[PPN]_2[Fe_2(CO)_6(\mu\text{-}SO_2)_2]\cdot 1NCCH_3$ (III). A red-orange crystal of **III** was mounted under N_2 on a Bruker SMART1000-CCD diffractometer. The intensity data were collected with 15 s frame times and interpreted with SAINT.[27] The initial unit cell parameters were determined from several frames of data, but were redetermined using all of the unique data. An absorption correction was applied with SADABS,[2] and the structure was solved and refined as a racemic twin, using SHELXTL. Hydrogen atoms were placed in idealized positions and refined with a riding model. Because of the method used by SADABS, no transmission factors are reported for the corrected data.

Results and Discussion

Reaction of $[MFe_3(CO)_{14}]^{2-}$ with SO_2. $[PPN]_2[MFe_3(CO)_{14}]$ (M = Cr, Mo, W) react with SO_2 to give CO, CO_2, $M(CO)_6$, $[PPN]_2[Fe_3(CO)_9(SO_2)]$ (**I**), $[PPN]_2[Fe_3(CO)_8(SO_2)S]$ (**II**), and other unidentified metal carbonyl compounds (eq 2). In contrast, $[HFe_3(CO)_9(SO_2)]^-$ (**VI**) is synthesized by the direct reaction of an excess of SO_2 with $[HFe_3(CO)_{11}]^-$. Reaction of $[Fe_3(CO)_{11}]^{2-}$ with SO_2 has been reported to produce a complex mixture of unidentified products.[28] Salts of dianions **I** and **II** were separated by partial solubility differences in 1:2 THF/ Et_2O. Previous research has shown that under an atmosphere of CO, heterometallic carbonyl clusters may undergo cleavage into lower nuclearity compounds.[29,30] In the current work, CO released by the replacement reaction by SO_2 leads to the formation of the thermodynamically stable homometallic carbonyls $M(CO)_6$ (M = Cr, Mo, W), along with iron−sulfur-containing carbonyl clusters. Excision of the heterometal also is seen in reactions of $[MFe_3(CO)_{14}]^{2-}$ where strong proton sources, such as HOTf, give $[HFe_3(CO)_{11}]^-$ and $Fe_3(CO)_{12}$ as products.[31] Similarly, $[Fe_3(CO)_{10}(COMe)]^-$ is obtained from reaction of $[MFe_3(CO)_{14}]^{2-}$ (M = Cr, W) with strong methylating agents, either MeOTf or $(CH_3)_3OBF_4$. In both reactions, the heterometal is lost as $M(CO)_6$.

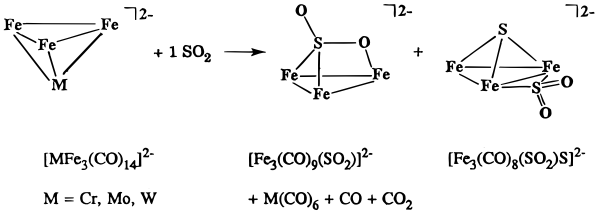

(2)

Reaction of **I** with additional SO_2 gives **II** in 48% yield (eq 3) plus CO_2. The formation of CO_2 may occur by transfer of oxygen from SO_2 to cluster bound carbonyl ligands, but the details of the reduction of SO_2 to sulfide ligand are uncertain.

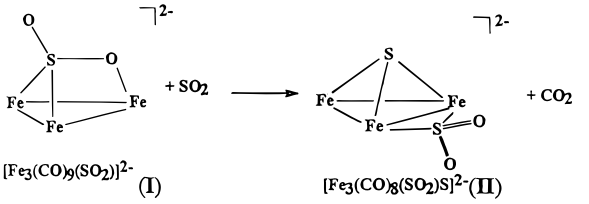

(3)

To the best of our knowledge, this is a rare example of CO

---

(21) Siemens *SAINT-PC*; Siemens, Ed.: Madison, WI, 1996.
(22) Sheldrick, G. M. *J. Appl. Crystallogr.*, in press.
(23) Sheldrick, G. M. *SADABS, Program for Absorption Correction of Area Detector Data*; Sheldrick, G. M., Ed.: Gottingen, Germany, 1996.
(24) Baur, W. H.; Kassner, D. *Acta Crystallogr.* **1992**, *B48*, 356−69.
(25) Marsh, R. E. *Acta Crystallogr.* **1997**, *B53*, 317−22.
(26) Flack, H. D. *Acta Crystallogr.* **1983**, *A39*, 876−81.
(27) Bruker *SAINT-NT*; Bruker, Ed.: Madison, WI, 1998.
(28) Karet, G. B. Unpublished results.
(29) Horwitz, C. P. Unpublished results.
(30) Geoffroy, G. L. *Acc. Chem. Res.* **1980**, *13*, 469−86.

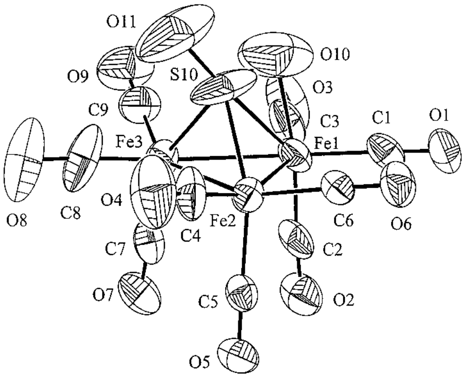

Figure 1. Thermal ellipsoid plot of $[Fe_3(CO)_9(SO_2)]^{2-}$ (**I**) at 30% probability.

Table 2. Selected Bond Lengths (Å) and Angles (deg) for $[PPN]_2[Fe_3(CO)_9(SO_2)]$ (**I**)

Fe1−C2	1.72(1)	Fe1−C3	1.77(1)
Fe1−C1	1.80(1)	Fe1−O10	2.14(1)
Fe1−S10	2.441(5)	Fe1−Fe3	2.605(2)
Fe1−Fe2	2.619(2)	Fe2−C6	1.748(8)
Fe2−C4	1.75(1)	Fe2−C5	1.791(8)
Fe2−S10	2.125(4)	Fe2−Fe3	2.615(2)
Fe3−C8	1.70(1)	Fe3−C9	1.71(1)
Fe3−C7	1.78(1)	Fe3−S10	2.157(4)
S10−O10	1.32(2)	S10−O11	1.55(1)
C1−O1	1.13(1)	C2−O2	1.18(1)
C3−O3	1.17(1)	C4−O4	1.15(1)
C5−O5	1.158(8)	C6−O6	1.154(8)
C7−O7	1.16(1)	C8−O8	1.18(1)
C9−O9	1.18(1)		
Fe1−Fe2−Fe3	59.70(4)	O10−S10−O11	115(1)
Fe1−Fe3−Fe2	60.23(4)	Fe1−C1−O1	175.7(8)
Fe2−Fe1−Fe3	60.07(4)	Fe1−C2−O2	174.6(7)
Fe1−S10−Fe2	69.6(1)	Fe1−C3−O3	175(1)
Fe1−S10−Fe3	68.7(1)	Fe2−C4−O4	176(1)
Fe2−S10−Fe3	75.3(1)	Fe2−C5−O5	176.9(7)
Fe1−S10−O10	86.4(7)	Fe2−C6−O6	176.1(6)
Fe2−S10−O10	116.9(7)	Fe3−C7−O7	178.5(7)
Fe2−S10−O11	115.1(7)	Fe3−C8−O8	176(1)
Fe3−S10−O10	116.1(8)	Fe3−C9−O9	178(1)
Fe3−S10−O11	112.9(6)		

acting as a reducing agent toward SO_2 in organometallic species. Another example is the reaction of SO_2 with $Cp_2Mo_2(CO)_6$ where CO from the molybdenum complex reduces SO_2 to give CO_2 and sulfido complexes.[10] Similarly, reaction of SO_2 with $CpMo(CO)_3H$ yielded $CpMo(CO)_3(SO_2H)$, CO, CO_2, SO_2, and COS. It is likely that the CO_2 is formed by oxidation of CO by SO_2 or the SO_2H derived species. In previous work, a reducing agent had to be added to elicit reduction of the SO_2 ligand, as shown in eq 1. For example, the reaction of $[HFe_3(CO)_9(SO_2)]^-$ (**VI**) with $NaPh_2CO$ yields the sulfur monoxide adduct, $[Fe_3(CO)_9(SO)]^{2-}$, while acetylation of the SO_2 ligand followed by reduction with $NaPh_2CO$ is required to form the sulfide cluster, $[Fe_3(CO)_9(S)]^{2-}$ (eq 1).[16] Intermediates are not typically seen or isolated in the reduction of SO_2 to lower sulfur oxides or elemental sulfur.[10] In the present work, we find that pure **I** reacts with SO_2 to give the partially reduced species **II**. Also, compound **I** reacts rapidly with 1 equiv of trifluoromethanesulfonic acid to give the known cluster $[PPN][HFe_3(CO)_9(SO_2)]$ (**VI**) in a quantitative yield.

The structure of **I**, Figure 1 and Table 2, is similar to that of $[HFe_3(CO)_9(SO_2)]^-$ (**VI**); both contain a μ_3,η^2-SO_2 and both have nine terminal carbonyls. The μ_3,η^2-SO_2 bonding mode for **I** gives rise to S−O stretches at 1162 and 902 cm^{-1} (Nujol) which are in the expected range.[10] The electron count in both **I** and **VI** can be understood if the S- and O-coordinated SO_2 ligand is counted as a four-electron donor. The S−O bond lengths for **I** are 1.55(1) Å for the exo oxygen and 1.32(2) Å for the metal bound S−O, and the O−S−O angle is 110.3(6)°. The protonated version of **I**, **VI**, has bond lengths of 1.62(1) Å for the exo and 1.434(9) Å for the metal bound S−O bonds, respectively, and a more open O−S−O angle of 119°. The S−O bond lengths for **I** are more typical of other η^2-sulfur dioxide compounds, where the uncoordinated, or exo, S−O bond is longer than the S−O bond which caps the trimetal face of the cluster.[2] Examples which follow the expected trend are $[Ru_3(CO)_9(SO_2)]^{2-}$ (S−O = 1.54(5) Å and 1.452(7) Å), $[Rh(CO)_4(SO_2)_3(P(OPh)_3)_4]$ (S−O = 1.47(1) Å, 1.44(2) Å, 1.43(2) Å, 1.50(2) Å),[32] and $[Pd(SO_2)_4(Ph_3As)_5]$ (S−O = 1.438(7) Å, 1.476(7) Å, 1.489(8) Å, 1.438(8) Å.).[33] Even though the structures of **I** and **VI** were determined at different temperatures, there are a few metric comparisons that are informative and statistically relevant. The hydride ligand in **IV** leads to a longer metal-bound S−O distance as well as an increase in the Fe−Fe bond length from 2.615(2) Å for **I** to 2.649(3) Å for **VI**. Also, Fe1−O10 is 0.10 Å longer than the Fe−O bond in **VI**.

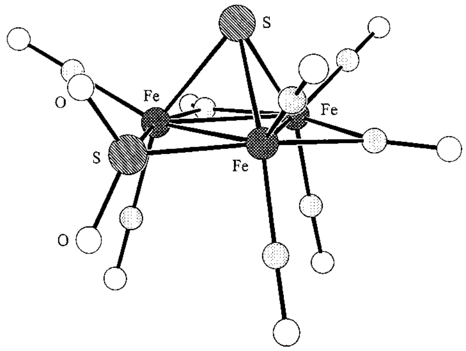

Figure 2. Proposed structure of $[Fe_3(CO)_8(SO_2)\ (\mu_3\text{-}S)]^{2-}$ (**II**).

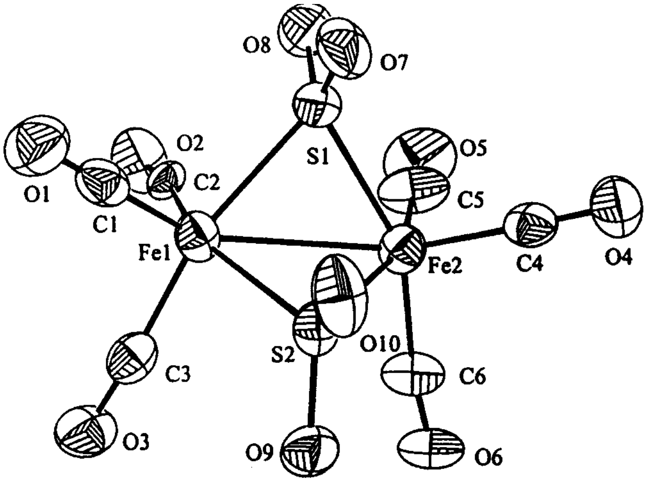

Figure 3. Thermal ellipsoid plot of $[Fe_2(CO)_6(SO_2)_2]^{2-}$ (**III**) at 50% probability.

Isotopically enriched **I** and **II** were prepared by stirring a methylene chloride solution of the cluster under an atmosphere of ^{13}CO. The ^{13}C NMR spectrum of $[PPN]_2[Fe_3(CO)_9(SO_2)]$ (**I**) shows fluxional behavior from 20 to −80 °C. At low

---

(31) Horwitz, C. P.; Shriver, D. F. *Adv. Organomet. Chem.* **1984**, *23*, 219−305.

(32) Briant, C. E.; Theobald, R. C.; Mingos, D. M. P. *J. Chem. Soc., Chem. Commun.* **1981**, 963.

(33) Burrows, A. D.; Mingos, D. M. P.; Powell, H. R. *J. Chem. Soc., Dalton Trans.* **1992**, 261.

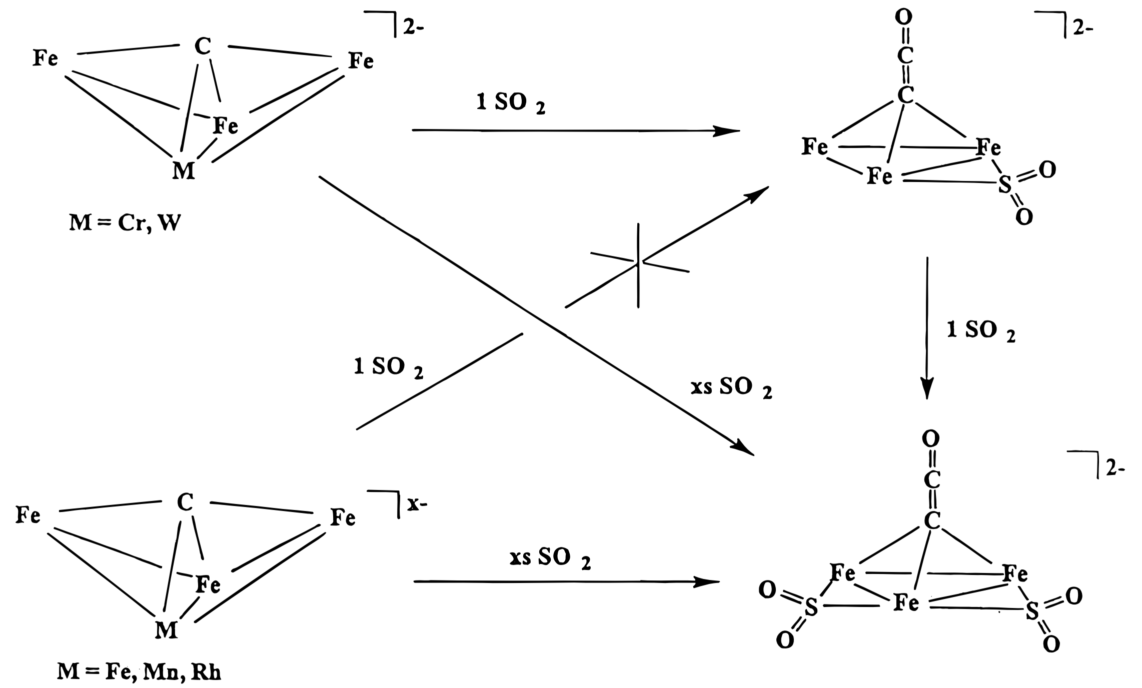

Figure 4. Reaction scheme for $[MFe_3(CO)_nC]^{2-}$ with SO_2.

temperatures, no peaks attributable to bridging carbonyls are present, in agreement with the solid state structure. At 20 °C, the metal carbonyl carbon resonances nearly coalesced to a single peak at 221.6 ppm. The ^{13}C NMR spectrum of $[PPN]_2[Fe_3(CO)_8(SO_2)S]$ (**II**) displays integrated intensities with a 2:2:4 ratio for edge-bridging carbonyls, carbonyls opposing the μ-SO_2, and carbonyls on iron adjacent to SO_2. No CO fluxionality was observed in the temperature range from 20 to −60 °C.

Several sets of data were collected on crystals of **II** with a SMART-CCD diffractometer, but the crystals diffracted weakly and the anion was disordered which resulted in a poor data set. The proposed structure for **II**, Figure 2, contains a μ_3-sulfide which acts as a four-electron donor and a μ-SO_2 which donates two electrons resulting in an electron precise cluster. The ν_{SO} stretch at 1066 cm^{-1} indicates the presence of a bridging SO_2 in the product, in agreement with the proposed structure.

The reaction of $[Fe_4(CO)_{13}]^{2-}$ with excess SO_2 produces $[Fe_2(CO)_6(SO_2)_2]^{2-}$ (**III**). This result is similar to observations with other iron−carbonyl clusters, where the iron−iron bond is easily cleaved by SO_2, leading to mono- and bimetallic compounds.[15] Red, translucent plates of $[PPN]_2[Fe_2(CO)_6(SO_2)_2]$ (**III**) were grown for the X-ray crystal structure determination by the slow diffusion of diethyl ether into an acetonitrile solution of **III**, and crystal data are presented in Table 1. The structure of **III**, Figure 3, contains two edge-bridging sulfur dioxide ligands, and the terminal carbonyls adopt an eclipsed configuration. A similar compound, $[Fe_2(CO)_8(SO_2)]$, prepared from iron nonacarbonyl, has one edge-bridging SO_2.[34−36] The Fe−Fe bond distance for **III** (2.621(3) Å) is significantly shorter than that of $[Fe_2(CO)_8(SO_2)]$ (2.717(4) Å) and slightly longer than the Fe−Fe bond distance for diiron nonacarbonyl (2.46 Å); additional bond length data are provided in Table 2. The O−S−O angles for **III** (110.2(3), and 110.2(4)°) are less than those for $[Fe_2(CO)_8(SO_2)]$ (113.9(7)°). The ^{13}C NMR spectrum of **III** displays a single carbonyl peak at 156 ppm from 20 to −80 °C.

Table 3. Selected Bond Lengths (Å) and Angles (deg) for $[PPN]_2[Fe_2(CO)_6(SO_2)_2]\cdot 1NCCH_3$

Fe1−Fe2	2.636(1)	Fe2−C4	1.788(8)
Fe1−C1	1.774(8)	Fe2−C5	1.799(7)
Fe1−C2	1.824(6)	Fe2−C6	1.813(7)
Fe1−C3	1.793(7)	Fe2−S1	2.235(2)
Fe1−S1	2.192(2)	Fe2−S2	2.203(2)
Fe1−S2	2.241(2)	C4−O4	1.143(8)
C1−O1	1.147(9)	C5−O5	1.146(8)
C2−O2	1.116(8)	C6−O6	1.116(9)
C3−O3	1.144(7)	S2−O9	1.482(6)
S1−O7	1.466(5)	S2−O10	1.463(5)
S1−O8	1.455(5)		
O7−S1−O8	110.2(3)	O9−S2−O10	110.2(4)
Fe1−C1−O1	178.0(7)	Fe2−C4−O4	179.0(6)
Fe1−C2−O2	169.7(6)	Fe2−C5−O5	172.0(7)
Fe1−C3−O3	176.0(7)	Fe2−C6−O6	178.1(8)
Fe1−S1−Fe2	73.08(6)	Fe1−S2−Fe2	72.77(6)
S1−Fe1−S2	83.30(7)	S1−Fe2−S2	83.17(7)

Reaction of $[MFe_3(CO)_nC]^{x-}$ + SO_2 (M = Cr, W: *n* =13, *x* = 2; M = Rh; *n* = 12, x = 1; M = Mn: *n* = 13, *x* = 1). Prior research in this group has shown that the reaction of 4 equiv of SO_2 with $[Fe_4(CO)_{12}C]^{2-}$ produces the bis-sulfur dioxide cluster **V** in 80% yield (Figure 4).[15] In the current investigation of the reaction of SO_2 with heterometallic, iron carbonyl clusters we find that 1 equiv of SO_2 reacts with $[PPN]_2[CrFe_3(CO)_{13}C]$ or $[PPN]_2[WFe_3(CO)_{13}C]$ to give the mono-sulfur dioxide adduct $[PPN]_2[Fe_3(CO)_8(SO_2)(CCO)]$ (**IV**).

Reaction of 4−6 equiv of SO_2 with $[MFe_3(CO)_nC]^{x-}$ (M = W, Cr, Rh, Mn, or Fe) produces the bis-SO_2 compound **V** as the only sulfur dioxide-containing product. Similarly, the mono-SO_2 adduct **IV** reacts with 1 equiv of sulfur dioxide to give the bis-SO_2 product **V**. Figure 4 summarizes the reactivity of heterometallic iron carbides with SO_2. In the reaction of the heterometallic, carbide clusters $[MFe_3(CO)_{13}C]^{2-}$ (M = W, Cr) with SO_2 the heterometal is extruded from the cluster as $M(CO)_6$. For the reactions of SO_2 with $[MFe_3(CO)_xC]^{x-}$ (M =

---

(34) Braye, D. E.; Hubel, W. *Angew. Chem., Int. Ed. Engl.* **1963**, *2*, 217−8.

(35) Meunier-Piret, J.; Van Meerssche, M. *Bull. Soc. Chim. Belg.* **1967**, *76*, 374−99.

(36) Field, D. S.; Newlands, M. J. *J. Organomet. Chem.* **1971**, *27*, 221−30.

Table 4. Raman Stretching Frequencies for Sulfur Dioxide Compounds

compound	ν_{CO} (cm^{-1})[a]	ν_{SO} (cm^{-1})[a]
$[Fe_3(CO)_9(SO_2)]^{2-}$	2013(m), 1914(s), 1892(vs), 1973(s, sh)	
$[Fe_3(CO)_8(SO_2)S]^{2-}$	2062(s), 1958(vs), 1918(m), 1903(m), 1842(m, br)[c]	
$[Fe_2(CO)_6(SO_2)_2]^{2-}$	1960(w), 1929(s), 1916(s), 1902(w)[c]	
$[Fe_3(CO)_7(SO_2)_2(CCO)]^{2-}$	2045(s), 1983(s), 1943(sh), 1924(vs) 1821(m)	
$[HFe_3(CO)_9(SO_2)]^{-}$	2068(s), 1966(vs), 1953(vs), 1910(m),[c] 2068(s)1973(vs), 1931(sh)[b]	
$[Fe_3(CO)_9(SO)]^{2-}$	2012(m), 1993(w), 1923(sh), 1897(vs), 1868(s)	
$[Fe_5(CO)_{13}(SO_2)]^{2-}$	2037(s), 1976(s), 1953(s), 1929(vs), 1897(s), 2041(s), 1976(sh), 1937(vs)[b]	
$[Fe_6(CO)_{15}C(SO_2)]^{2-}$	2038(s), 1955(sh), 1943(vs), 1931(sh)	1046(s)
$[Ru_3(CO)_9(SO_2)]^{2-}$	2044(s), 2003(m), 1976(vs), 1956(vs), 1845(w, br)[c]	1055(m)
$[Ru_3(CO)_7(SO_2)_3]^{2-}$	2060(w), 2044(s), 2002(sh), 1965(vs), 1950(sh), 1840(w,br)[c]	1056(m)

[a] Solid sample, all as $[PPN]^+$ salts. [b] CH_2Cl_2. [c] Sample fluoresces.

Mn, Rh), the fate of the heterometal cluster was not determined. A mono-SO_2 compound is not observed in our reaction of 1 equiv of SO_2 with $[Fe_4(CO)_{12}C]^{2-}$; instead the only products are the known compound $[PPN]_2[Fe_3(CO)_7(SO_2)_2(CCO)]$ (**V**)[15] and the starting material $[Fe_4(CO)_{12}C]^{2-}$.

Characterization of $[PPN]_2[Fe_3(CO)_8(SO_2)(CCO)]$ (IV). Clear, dark red crystals of $[PPN]_2[Fe_3(CO)_8(SO_2)(CCO)]$ (**IV**) were grown from a THF solution layered with Et_2O. Several attempts were made to determine the X-ray crystal structure of **IV** (with $[PPN]^+$ and $[Et_4N]^+$ as counterions); however, both structures appeared to be severely disordered. The rough structural parameters from the X-ray data indicate an edge-bridging SO_2 and two edge-bridging carbonyls. Infrared spectra for **IV** indicate a bridging carbonyl with a stretching frequency at 1774 cm^{-1} in solution. An IR spectrum of **IV** contains an S−O stretching frequency at 1020 cm^{-1}, and in a Nujol mull ν_{SO} bands are present at 1064 and 1020 cm^{-1}, indicating an S-bound bridging SO_2,[10] where SO_2 is acting as a two-electron donor. The higher π acidity of SO_2 compared to that of CO is evidenced by the higher carbonyl stretching frequencies when SO_2 is substituted for CO. In the series $[Fe_3(CO)_9(CCO)]^{2-}$, **IV**, and **V** which contain 0, 1, and 2 bridging SO_2 ligands, ν_{CO} shifts to higher frequencies by approximately 20 cm^{-1} for each SO_2 substitution.

A ^{13}C-enriched sample of $[PPN]_2[WFe_3(^{13}CO)_{13}13C]$ was allowed to react with SO_2, and a ^{13}C NMR of the resulting product, **IV**, indicates fluxional behavior between −120 °C and room temperature. Below −40 °C, the integrated intensities of the CO ligands are in the expected 2:1:1:2:2 ratio. The α and β carbons of the −CCO ligand are present at 165.6 and 2.2 ppm, respectively, and show J_{C-C} of 45.4 Hz. The ^{13}C NMR signal for the α-carbon of CCO is not observed above −20 °C. When **IV** is heated above 35 °C, unidentified products result.

Raman Study. Raman stretching frequencies for several sulfur oxide-containing clusters are shown in Table 4. These spectra were collected on a FT instrument with 1064 nm excitation. Several of the samples were weakly fluorescent, while others decomposed under high laser intensities, making it difficult to obtain meaningful information. The S−O stretching frequencies were observable with all of the triruthenium clusters, despite the fluorescence. Among the iron clusters, S−O stretches were observed in the Raman spectrum only for $[Fe_6(CO)_{15}(C)(SO_2)]^{2-}$. Vibrations due to the $[PPN]^+$ cations may obscure some of the S−O stretches. The observed Raman stretching frequencies are identical to the infrared stretching frequencies.

Summary

The reaction of SO_2 with $[MFe_3(CO)_{14}]^{2-}$ (M = Cr, Mo, W) result in loss of the heterometal and formation of triiron SO_2- and S-containing clusters. Similarly, the reaction of SO_2 with $[Fe_4(CO)_{13}]^{2-}$ results in cluster degradation and formation of the new bimetallic $[Fe_2(CO)_6(SO_2)_2]^{2-}$. The new ketenylidene compound, $[Fe_3(CO)_8(SO_2)(CCO)]^{2-}$, is formed in the reaction of 1 equiv of SO_2 with $[MFe_3(CO)_{13}C]^{2-}$ (M = Cr, W). The known compound $[Fe_3(CO)_7(SO_2)_2(CCO)]^{2-}$ is the product of the reaction of an excess of SO_2 with $[MFe_3(CO)_nC]^{x-}$ (M = Mn, Cr, W, Rh). The compound $[Fe_3(CO)_9(SO_2)]^{2-}$ (**I**) was identified as an intermediate in the formation of $[Fe_3(CO)_8(SO_2)S]^{2-}$ (**II**). This is a rare example in metal carbonyl cluster chemistry where CO acts as a reducing agent toward SO_2 to give a sulfido species.

Acknowledgment. We thank Susie Miller of Colorado State University, Charlotte Stern of Northwestern University, and Scott Wilson of the University of Illinois for their collection of crystallographic data. C.C.R. and T.E.A.S. thank Prof. J. A. Ibers for helpful discussions regarding the crystal structure determinations. We also thank G. Kubas of Los Alamos National Laboratory for helpful discussions. The research was sponsored by the Department of Energy grant DE-FG02-86ER13640.

Supporting Information Available: X-ray crystallographic files in CIF format for the structure determinations of $[PPN]_2[Fe_3(CO)_9(\mu_3,\eta^2\text{-}SO_2)]$ (**I**), $[PPN]_2[Fe_3(CO)_8(\mu\text{-}SO_2\ (\mu_3\text{-}S))]$ (**II**), and $[PPN]_2[Fe_2(CO)_6(\mu\text{-}SO_2)_2]$ (**III**). This material is available free of charge via the Internet at http://pubs.acs.org.

IC980762J